I. Cesium Leaching in CsA and CsX Zeolites

Enrique J. Lima,*,† Ilich A. Ibarra,† Marco A. Vera,† Victor H. Lara,† Pedro Bosch,‡ and Silvia Bulbulian§

Universidad Autónoma Metropolitana, Iztapalapa, A. P. 55-532, Av. San Rafael Atlixco No. 186 Col. Vicentina, 09340 México D.F., Mexico, Instituto de Investigaciones en Materiales, A. P. 70−360, Universidad Nacional Autónoma de México, Circuito Exterior, Ciudad Universitaria, 04510 México D. F., Mexico, and Instituto Nacional de Investigaciones Nucleares, A. P. 18-1027, Col. Escandón, Delegación Miguel Hidalgo, 11801 México D. F., México.

Received: March 24, 2004

Sodium zeolite X and sodium zeolite A have been exchanged with cesium solutions prepared from three cesium salts (chloride, nitrate, and acetate). Depending on the solution, the cesium cations were found to be located in different sites of the zeolite networks. If cesium acetate solution is used, then cesium reaches sites SII and SIII in the large cavity whereas if nitrate or chloride solutions are put in contact with zeolites, cesium is positioned only in sites SIII. This distribution determines the leaching behavior of the studied zeolites. When the samples were thermally treated to encapsulate partially the cesium cations, it was found that their behavior was different from the one observed in a previous work on cobalt exchanged X and A zeolites

Introduction

In the nuclear industry, ion exchange is widely used to remove radioactive metal ions from solutions either with resins, clays or zeolites.[1−4] The retained radionuclides may then leach and, of course, such leakage into the environment has to be avoided. Nuclear wastewaters are conventionally circulated through columns containing the ion-exchanging materials. Unfortunately, clays present a low exchange capacity and resins are unstable in the pH conditions often required and because of their radiolytic decomposition. Instead, zeolites exhibit a high exchange capacity and an easy availability (natural or synthetic) as they are also used in catalysis,[5] the detergent industry,[6] or as a building material[7] among other applications.

Each type of zeolite is selective for a unique ion and rarely traps more than one simultaneously.[8] Zeolite A, which has a silicon-to-aluminum ratio of 1, has a high equilibrium selectivity for alkaline earth cations, and therefore, it is often used to remove radioactive strontium from wastewaters.[9] Zeolite X, instead, prefers lithium, sodium, and potassium and therefore it is often used as catalyst.[10]

The shape selectivity of zeolites, due to the free diameters of their pores and cages, strongly depends on the cation distribution in the zeolite lattice. If the temperature is increased, the zeolite cations are not rigidly located at their position and they present a rather high mobility.[11] We selected zeolites A and X as they have a very different exchange capacity although, structurally they only differ on the way the cubooctahedra cages are assembled. Their largest pore diameters are for sodium zeolite A: 0.36 nm and for sodium zeolite X: 0.85 nm.

These zeolites retain fission products as ^{137}Cs whose half-life is 34 years. The irradiation effect may develop defects in the cesium zeolite network and modify it structurally with cracks due to the creation of paramagnetic centers. Cesium may then diffuse to contaminate the environment. To avoid this problem, conventionally, the exchanged materials are thermally treated to obtain a homogeneous vitreous solid.[12]

Zeolites, depending on their structure, present different adsorption sites which may be occupied by cesium. When the crystallinity of the exchanged zeolite diminishes, the weakest bonds are destroyed first. Therefore, if cesium is positioned in a weak crystallographic site, then it should be occluded, but if it is close to a well-structured zone, it may remain in the residual zeolite. Cesium, as a cation in solution, is surrounded by a corresponding number of anions that may have a strong effect on the positioning of cesium. Anions can alter the pH, modify the viscosity, and therefore, the diffusion of cations among other factors.

In a previous paper, we reported that the destruction of A or X zeolite by thermal treatment is a good strategy to occlude cobalt ions and limit their leaching. Furthermore, we found that γ-irradiation favored the occlusion of waste atoms.[13] Still, to substitute the thermal treatment step, Dyer and Abou-Jamous have proposed a secondary ion exchange adsorbing a large cation to block the release of the radioisotopes.[14]

In this work, we report on the effects of the thermal treatments on the cesium exchanged zeolites prepared from aqueous solutions of different salts. Therefore, we are studying the effect of anions on cesium location in the zeolite A and X networks and the effect of thermal treatment in both series of solids.

Experimental Procedures

Materials. Zeolites NaA and NaX with a framework Si/Al ratio of 1.2 and 1, respectively, were supplied by Union Carbide, type 4A and Sigma Chemical Company, particle diameter less than 10 μm. The other reagents were commercial analytical grade and they were used without further purification.

Exchange Procedure. Five-gram samples of NaA or NaX were shaken for 3 h in 100 mL of 0.1 N solution of CsCl,

* To whom correspondence should be addressed. E-mail: lima@xanum.uam.mx. Fax: (525) 58-04-4666. Phone: (525) 58-04-4667.
† Universidad Autónoma Metropolitana.
‡ Instituto de Investigaciones en Materiales, A. P. 70−360, Universidad Nacional Autónoma de México, Circuito Exterior, Ciudad Universitaria.
§ Instituto Nacional de Investigaciones Nucleares.

10.1021/jp048683i CCC: $27.50
Published on Web 07/10/2004

$CsNO_3$, or $CsOOC_2H_3$ for 3 h. Then, the solids were separated by centrifugation and washed with deionized water. The samples that were exchanged with the CsCl solution are referred to in this paper as CsX-1 or CsA-1, the samples that were exchanged with the $CsNO_3$ solution are labeled as CsX-2 or CsA-2 and finally, the solids denoted as CsX-3 or CsA-3, correspond to samples exchanged with the $CsOOC_2H_3$ solution.

Thermal Treatment. The ZA samples were thermally treated at 1073 K, and the X samples were treated at 973 K. In our previous work,[9] we found that the sodium or cobalt A zeolites treated at 1073 K recrystallized as nepheline and carnegeite. Instead sodium and cobalt X zeolites are unstable at temperatures of 973 K. We chose these temperatures to study first the behavior of a recrystallized zeolite, zeolite A. In cobalt exchanged X zeolite, we found that with irradiation and thermal treatment (973 K) the Co leaching was reduced 20%. Therefore, local vitrification seems to have started at this temperature. Our purpose was to study the performance of this same zeolite exchanged with cesium compared on one hand with the cobalt zeolite and on the other hand with the carnegeite−nepheline.

Neutron Activation Analysis. The samples were irradiated in a Triga Mark III nuclear reactor for 15 min with an approximate neutron flux of 10^{13} n/cm^2 s. The 0.605 MeV photo peak from ^{134}Cs produced by the nuclear reaction ^{133}Cs (n, γ) ^{134}Cs was measured with a Ge/hiperpure solid-state detector coupled to a computerized 4096-channel pulse analyzer.

X-ray Diffraction. The zeolite samples were studied by X-ray diffraction. A Siemens D5000 powder diffractometer with a copper anode tube was used. The K_α radiation was selected with a diffracted beam monochromator. The cell parameters were obtained using a corundum (α-Al_2O_3) standard to correct the (642) peak shift for the X zeolites and the (321) peak for the A zeolites.

The radial distribution functions were calculated from the full diffraction patterns as shown by Magini and Cabrini.[15] A molybdenum anode X-ray tube was used to reach the required high values of the angular parameter $h = (4\pi\sin\theta)/\lambda$, and the diffractogram was measured by step scanning at angular intervals of 0.08°.

NMR Spectroscopy. The MAS NMR spectra were performed on a Bruker ASX-300 spectrometer at a resonance frequency of 39.37 MHz for ^{133}Cs. All of the spectra were recorded after single pulse excitation with repetition times of 1 s. The spectra were carried out with sample spinning rates of 5 kHz. The chemical shifts were referenced to a 1.0 M aqueous solution of CsCl.

To collect the NMR spectrum data, the heated samples were immediately placed in a glovebox under dry N_2 and were packed in ZrO_2 rotors. The time for recording one NMR spectrum was not longer than 10 min.

The ^{27}Al MAS NMR spectra were obtained operating the spectrometer at 78.21 MHz. Pulse width was 2 μs. The spinning rate was 10.0 kHz.

FTIR Spectroscopy. The FTIR spectra of samples, as pellets with CsI, were obtained at room temperature on a Perkin-Elmer (Spectrum 2000) spectrometer, which was equipped with a FR-DTGS detector. The spectral resolution was 2 cm^{-1}.

Cesium Leaching. Cesium exchanged zeolites were tested for Cs^+ desorption shaking them in contact with 1 N NaCl solution for 2 h. Solids and liquids were then separated by centrifugation, and the desorbed Cs^+ present in the NaCl solution was determined by neutron activation analyses.

TABLE 1: Cesium content in the exchanged A and X zeolites as determined by nuclear activation

sample	cesium content (meq Cs/g zeolite)
CsA-1	1.10 ± 0.05
CsA-2	1.09 ± 0.04
CsA-3	1.00 ± 0.05
CsX-1	1.10 ± 0.05
CsX-2	1.20 ± 0.05
CSX-3	1.25 ± 0.06

TABLE 2: Comparison of Cell Parameters (Å) in Zeolites A and X before and after Cesium Exchanged

	original zeolite	Cs zeolite-1	Cs zeolite-2	Cs zeolite-3
zeolite A	12.16	12.23	12.27	12.25
zeolite X	24.80	24.91	24.93	24.89

TABLE 3: Comparison of Interatomic Distances in Zeolites NaA and NaX as Determined by the Radial Distribution Function

sample	(Al, Si)−O	O−O; (Al, Si)−Si	(Si, Al)−O	Na−O Si−O
Na−ZA	1.67	3.12	4.15	5.1
Na−ZX	1.67	3.11	4.20	5.0

Results

Neutron Activation Analysis. The content of cesium in each zeolite as determined by neutron activation analyses is reported in Table 1. Only one exchange step was performed.

X-ray Diffraction of Cs-Exchanged Zeolites. The X-ray diffraction patterns of sodium and cesium exchanged zeolites A are compared in Figure 1. The patterns correspond to fully crystalline zeolites and no cesium compounds were detected. The exchange of the sodium cations by cesium is confirmed by the relative intensities of the X-ray diffraction peaks. The peaks with interplanar distances d = 12.28, 7.08, and 4.35 Å diminish and those with 3.56 and 3.08 Å increase.

Similar results are found for the sodium and cesium zeolites X as, with cesium exchange, X-ray diffraction peaks with d = 5.73, 4.41, 4.16, and 3.69 Å decrease and those with d = 7.21 and 6.24 Å increase. The cell parameters are the same for CsA-1, CsA-2, and CsA-3 within error range and for CsX-1, CsX-2, and CsX-3 samples a_0 was 12.25 and 24.91 Å respectively, Table 2

Table 3 compares the position of the first peaks present in the radial distribution functions of sodium A and sodium X zeolites. They are located at the same radial distances showing that the interatomic distances corresponding to the first neighbors are similar, they correspond indeed to the distances present in the primary silicon−oxygen tetrahedra. The peaks were assigned following the reported theoretical results.[16] Thus, with cesium exchange (only the CsA-2 and CsX-2 samples were studied), the positions of those first three peaks present in the radial distribution function of the zeolites should not be altered as they correspond to structural distances of the aluminosilicate, only the distance oxygen−cesium should be superimposed. The distance Cs^+−O^{2-} is 3.12 Å. This value falls at the same position, in the radial distribution function, as the distances corresponding to O−O or (Al, Si)−O, in both zeolites, and, therefore, it should not be resolved.

In zeolite A, as expected, the location of the first three peaks is not altered. Only the long range order is modified. With cesium exchange the peak at 0.51 nm fades out (this peak may be attributed to second neighbors of the bond Na−O and new peaks at 0.58 and 0.69 nm appear, probably due to the cesium−oxygen second and third neighbors, Figure 2.

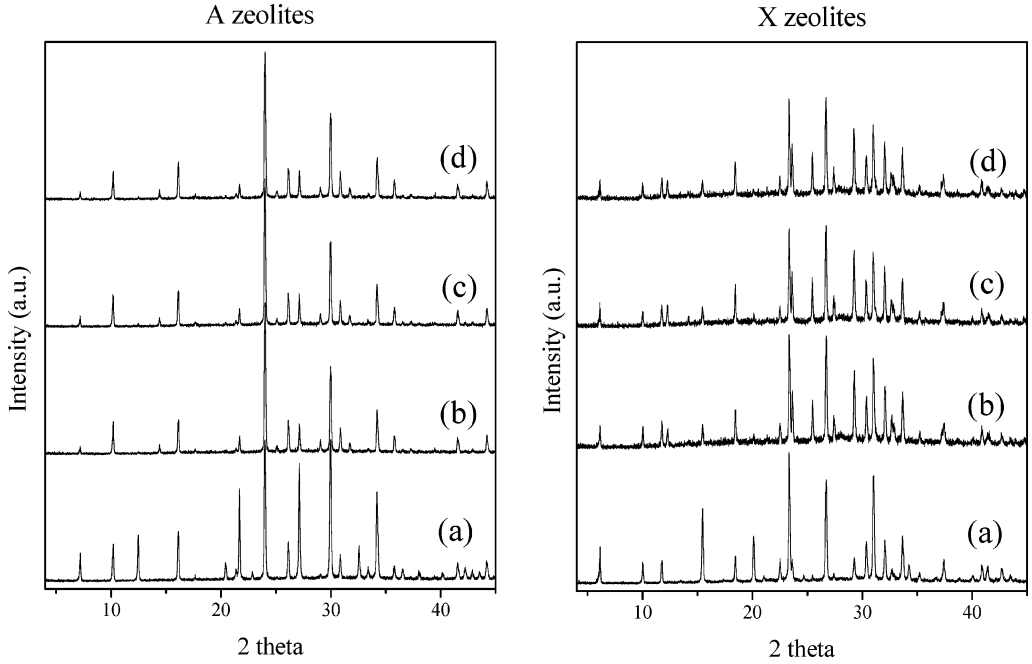

Figure 1. X-ray diffraction patterns of sodium and cesium A and X zeolites. (a) NaA, NaX; (b) CsA-1, CsX-1; (c) CsA-2, CsX-2; and (d) CsA-3, CsX-3.

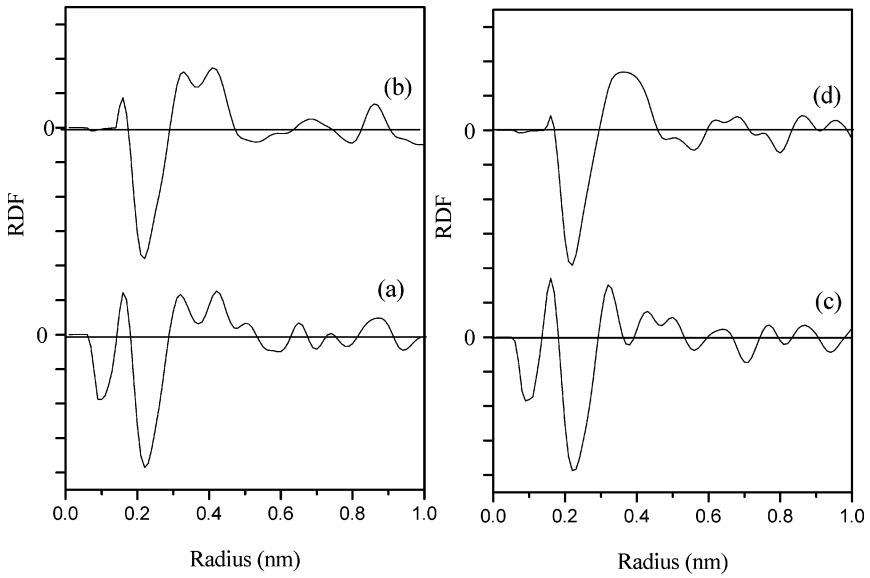

Figure 2. Radial distribution functions of zeolites (a) NaA, (b) CsA-2, (c) NaX, and (d) CsX-2.

Instead, in cesium exchanged zeolite X, the second and third peaks are not resolved, only a very broad peak (from 0.312 to 0.410 nm) is observed, we conclude, then, that the distance cesium oxygen is not as well defined as in zeolite A. Again, with cesium exchange, the peak at 0.50 nm in the original X zeolite diminishes and a peak at 0.69 nm, that can be attributed to a Cs−O (third neighbors) distance, is observed.

NMR of Cesium Exchanged Zeolites. Figure 3 includes ^{133}Cs MAS NMR spectra for unheated samples. Although the spectra for CsX-1 and CsX-2 samples exhibit only one peak at −88 ppm, the spectrum for CsX-3 presents two peaks at −86 and −70 ppm. The resonances close to −88 and −70 ppm are assigned to cesium located in III and II sites, respectively.[17,18] Note that both sites occupied by cesium are into the large cavities.

All samples in CsA series present only one resonance at −45 ppm. As no assignation of cesium resonances in zeolite A have been reported, data for zeolite A, in this work, are attributed comparing them with those obtained for zeolite X.

Deconvolution of ^{133}Cs MAS NMR spectra was carried out, and the integrated intensities of the isotropic resonance are reported in Table 4. On one hand, isotropic line shapes can be assumed as the cesium cations ($I = 7/2$) present weak quadrupolar interactions with zeolite structure.[19] On the other, all resonances reported in Table 4 exhibit spinning sidebands (Figure 3). Then, for ^{133}Cs nucleus the isotropic resonances are assumed to contain the intensity from the central transition and the satellite transitions included in the spinning sidebands. Norby et al.[18] have shown that the ^{133}Cs NMR intensities are directly correlated with populations of cesium in the sites of zeolites. Therefore, in this study, the relative population of cesium in the various sites of zeolite A and zeolite X is directly proportional to the integrated intensities, Table 4.

FTIR of Cesium Exchanged Zeolites. Figure 4 shows the FTIR spectra of the nonheated cesium zeolites, A and X. No

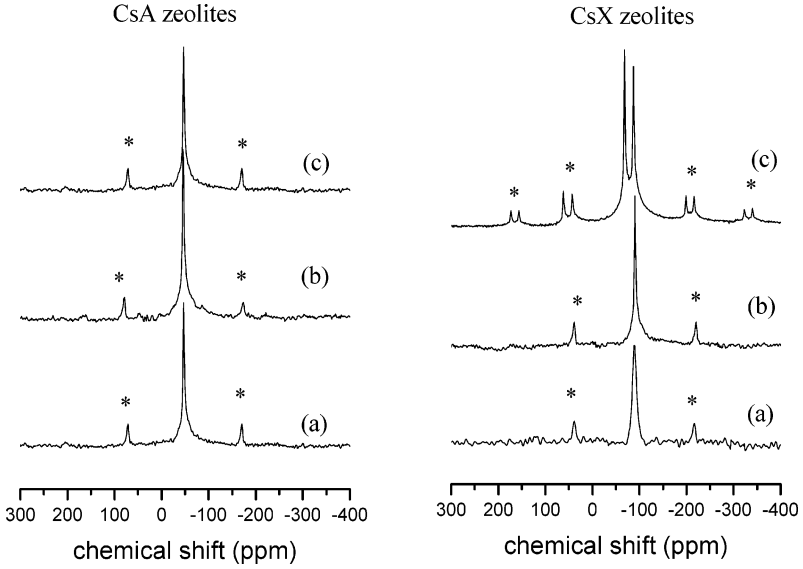

Figure 3. ^{133}Cs MAS NMR spectra of cesium A and X zeolites. (a) CsA-1, CsX-1; (b) CsA-2, CsX-2; and (c) CsA-3, CsX-3. Peaks labeled * are the spinning sidebands.

TABLE 4: Population Cesium in the Unheated and Heated Cs/Zeolites as Determined by Their Relative Signal Intensities in the ^{133}Cs MAS NMR Spectra

T (K)	site	CsX-1	CsX-2	CsX-3	CsA-1	CsA-2	CsA-3
298	SIII	1.0	1.0	0.42	1.0	1.0	1.0
	SII	0.0	0.0	0.58	0.0	0.0	0.0
	SII′	0.0	0.0	0.0	0.0	0.0	0.0
	SI′	0.0	0.0	0.0	0.0	0.0	0.0
673	SIII	0.57	0.59	0.41	0.43	0.43	0.4
	SII	0.33	0.29	0.27	0.31	0.29	0.29
	SII′	0.11	0.12	0.22	0.27	0.27	0.31
	SI′	0.0	0.0	0.09	0.0	0.0	0.0
973/1073	SIII	0.49	0.53	0.33	0.0	0.0	0.0
	SII	0.29	0.17	0.26	1.0	1.0	1.0
	SII′	0.11	0.12	0.32	0.0	0.0	0.0
	SI′	0.11	0.18	0.09	0.0	0.0	0.0

TABLE 5: Population Cesium in the Leached and Dry Cs/Zeolites as Determined by Their Relative Signal Intensities in the ^{133}Cs MAS NMR Spectra

T (K)	site	CsX-1	CsX-2	CsX-3	CsA-1	CsA-2	CsA-3
298	SIII	0.71	0.79	0.51	0.89	0.89	0.85
	SII	0.29	0.21	0.49	0.11	0.11	0.16
	SII′	0.0	0.0	0.0	0.0	0.0	0.0
	SI′	0.0	0.0	0.0	0.0	0.0	0.0
673	SIII	0.65	0.67	0.4	0.40	0.36	0.31
	SII	0.20	0.17	0.21	0.25	0.25	0.28
	SII′	0.15	0.16	0.28	0.34	0.39	0.41
	SI′	0.0	0.0	0.13	0.0	0.0	0.0
973/1073	SIII	0.49	0.51	0.74	0.0	0.0	0.0
	SII	0.20	0.16	0.22	1.0	1.0	1.0
	SII′	0.14	0.15	0.40	0.0	0.0	0.0
	SI′	0.15	0.20	0.12	0.0	0.0	0.0

differences are observed for each group of zeolites. Note that in the CsA-3 and CsX-3 samples, the band close to 1570 cm^{-1} due to an asymmetric CO stretch absorption is not observed. Then, the samples do not exhibit any remaining cesium acetate. The IR absorption bands that might be attributed to interactions between cesium cations and zeolitic sites were not observed since these characteristic frequencies generally occur in the far-infrared spectral window.

X-ray Diffraction of Thermally Treated Zeolites. The zeolite A heated at 1073 K is partially destroyed. The X-ray diffraction peaks present in the pattern may be attributed to the following crystalline compounds: zeolite A, nepheline, carnegeite and quartz, Figure 5. In cesium exchanged zeolite X, the structure was maintained up to 973 K.

Figure 6 compares the radial distribution functions of the cesium exchanged samples treated at 973 and 1073 K. The radial distribution function of the samples CsA-2 treated at 973 K is most interesting as the peaks are much more defined revealing a more structured material. The cesium−oxygen distance, initially at 0.69 nm in the sample treated at 1073 K, is now at 0.66 nm. If the sample is treated at 1073 K, the peaks fade out, the long-range order is lost and only the main distances corresponding to the aluminosilicate remain.

For comparison purposes, the zeolite X was heated to 1073 K to be sure that the zeolite network collapsed, and hence that the radial distribution functions were sensible to crystallinity. In zeolite X, the effect of temperature is clear: the initial order is lost and the material loses its structure, it becomes amorphous. The radial distribution functions reveal that zeolite X treated at 1073 K is less ordered than the zeolite A treated at the same temperature, as the peaks at distances larger than 0.5 nm are more undefined. Still, it is interesting to note that the second and third peaks are resolved in the 1073 K treated sample showing that cesium−oxygen distance is now well defined and coincides with the O−O distance. Again, in these samples, the main conclusion is that cesium−oxygen distance varies as the temperature is increased, most probably because the cesium occupies different positions in the zeolite network or in vitreous material.

FTIR Spectra of Thermally Treated Zeolites. The infrared study, Figure 7, of the uncalcined and calcined samples is in agreement with the X-ray diffraction results. When the samples are calcined, the main modification of the FTIR spectra is, in the group of zeolites CsA, that the band at 375 cm^{-1} fades out at 1073 K, this band was assigned by Flanigen et al.[20] to the pore opening of external linkages. However, a very recent work[21] assigned the band to the 4R opening vibration. From both assignments we conclude that, if the band is observed, zeolite entities are present.

In the CsA zeolites, the band 6R pore-opening vibration disappears at 1073 K, due to alumina formation with the consequent framework collapse. The segregation of alumina was not observed by diffraction studies but the ^{27}Al NMR spectra show that a fraction of tetrahedrically coordinated aluminum

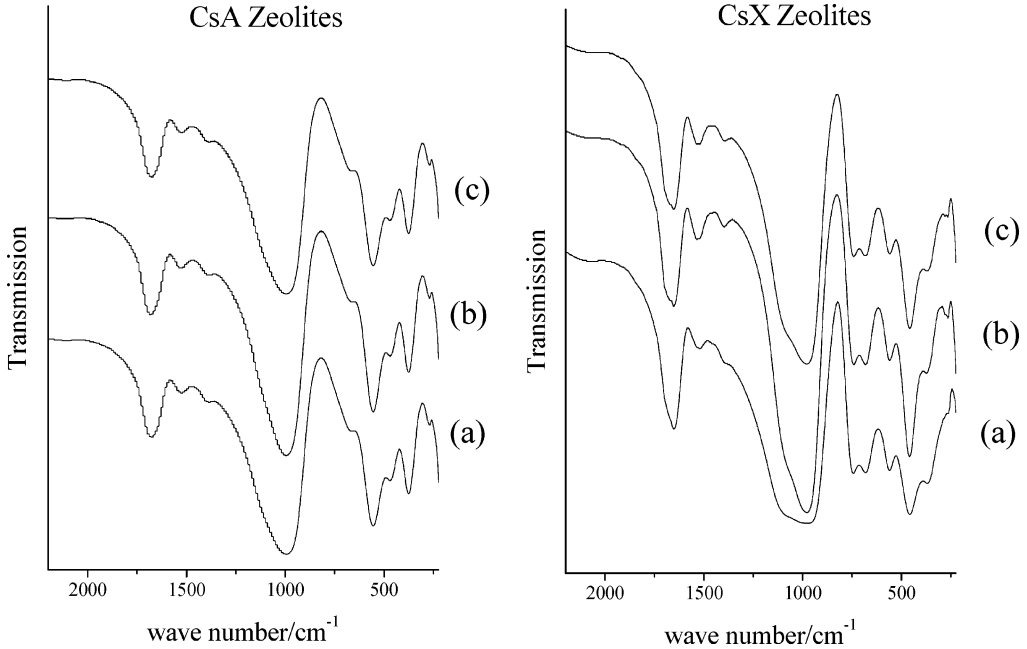

Figure 4. FTIR Spectra of cesium zeolites (a) CsA-1, CsX-1; (b) CsA-2, CsX-2; and (c) CsA-3, CsX-3.

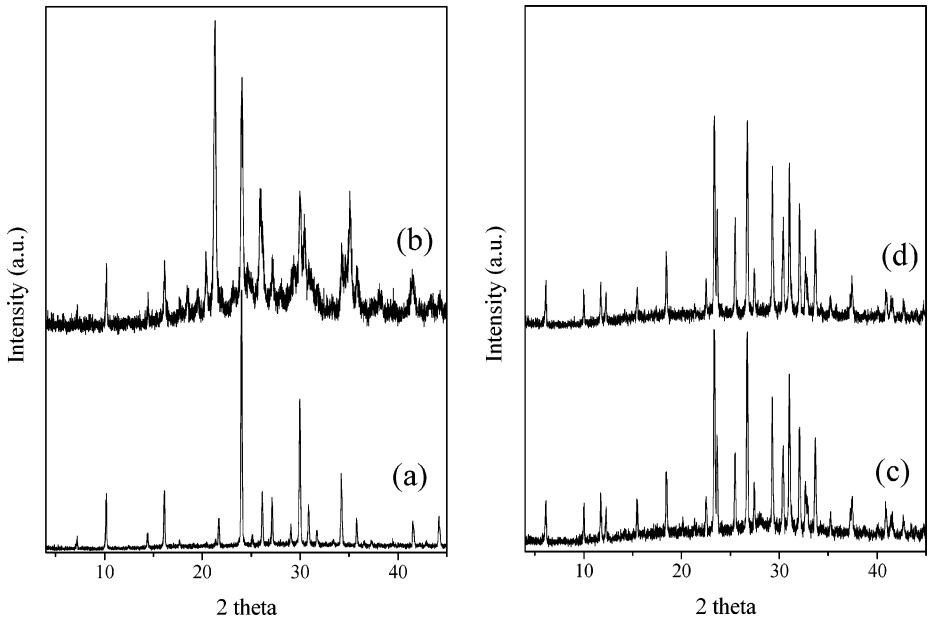

Figure 5. X-ray diffraction patterns of (a) CsA-2 unheated, (b) CsA-2 heated at 1073 K, (c) CsX-2 unheated, and (d) CsX-2 heated at 973 K.

atoms (peak at 54 ppm) turns out to be octahedrically (signal close to 0 ppm) coordinated as in alumina, Figure 8. In FTIR spectra for CsX samples, the bands due to 6R and 4R pore opening are observed as far as the zeolitic structure is maintained. However, in the corresponding ^{27}Al NMR spectrum, the amount of octahedral aluminum species observed, Figure 8, is not enough to produce the zeolite lattice collapse.

NMR of Thermally Treated Zeolites. When the various exchanged zeolite X samples are heated at 973 K, a similar distribution of cesium cations is obtained for CsX-1 and CsX-2 samples, i.e., 80% in large cavities and 20% in sodalite cages, but the cesium in CsX-3 sample is again differently distributed (60% in large cavities and 20% in sodalite cages), Table 4.

Spectra of samples of CsA series, heated at 1073 K, present only one peak at −60 ppm. Remember that CsA samples heated at 1073 K are a mixture of nepheline, quartz, and A zeolite. The unique resonance observed is close to resonances observed for cesium in zeolite A. However, amorphous material is most probably an aluminosilicate where the cesium can be located in symmetric sites as in zeolite. Cesium leaching results discussed below support this hypothesis.

Cesium Leaching. The cesium leaching curves, as determined by neutron activation analysis are shown in histograms of Figure 9a and 9b. In zeolite A, cations are located always in similar positions as shown by NMR results. Hence, CsA-1, CsA-2, and CsA-3 samples follow the same trend. With temperature, in all cases, the cesium retention is increased from ca. 75% at 298 K to ca. 85% at 1073 K. High cesium retention in CsA samples heated at 1073 K may be attributed to the zeolite structure collapse. Nepheline, quartz, and amorphous material are formed although some zeolite A remains.

Instead, samples CsX-1 and CsX-2 (zeolite X exchanged with CsCl and $CsNO_3$) retain 80% of the initial amount of cesium; but in CsX-3 sample (exchanged with $CsOOCCH_3$) the retained amount is lower, 73%. Samples heated at 673 or 973 K reproduce this leaching tendency, cations are again positioned

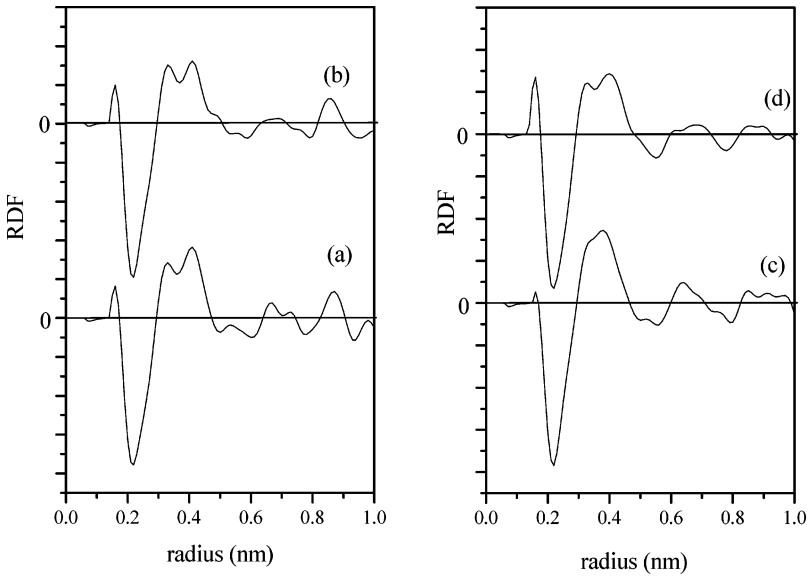

Figure 6. Radial distribution functions of (a) CsA-2 treated at 700 °C, (b) CsA-2 treated at 800 °C, (c) CsX-2 treated at 700 °C, and (d) CsX-2 treated at 800 °C.

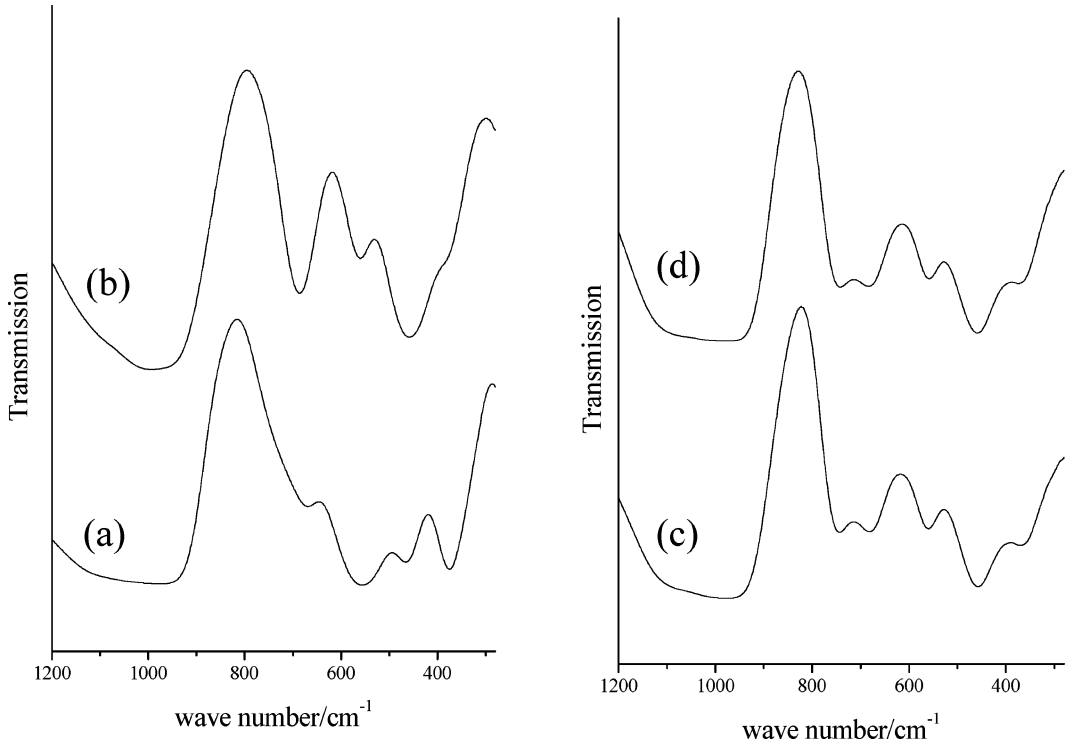

Figure 7. FTIR spectra of (a) CsA-2 unheated, (b) CsA-2 heated at 1073 K, (c) CsX-2 unheated, and (d) CsX-2 heated at 973 K.

in different sites in CsX-3 sample. Note that samples heated at 673 K retain less than samples at 298 K. This diminution may be attributed to cesium location. In samples treated at 298 K, most cesium in CsX-1 and CsX-2 is in position III but in CsX-3, it is distributed between sites II and III. With temperature (673 K), samples CsX-1 and CsX-2, cesium reaches sites II but in CsX-3 the four sites are occupied (III, II, II′, and I′). The distribution of cesium in the zeolites after leaching is presented in Table 5 as determined by NMR.

Discussion

Our results may be summarized as follows. The cesium content in both zeolites is close to 1 meq/g independently of the initial cesium salt. In zeolite A, no effect of the initial salt on the location of cesium ions is found but in zeolite X cesium is located in sites II and III if the initial salt is CsCl or $CsNO_3$, and more cesium is in position SII when the initial salt is $CsOOC_2H_3$. Cell parameters are insensitive to cesium exchange. As the cell parameters are not altered in the echanged zeolites, the amount of cesium retained agrees with the equilibrium exchange isotherms at 298 K reported by Barrer et al.[22]

From radial distribution functions, it seems that in zeolite A, cesium atoms are localized, and the distance cesium oxide is well-defined. As zeolite A has as many aluminum atoms as silicon atoms, the number of exchange sites is very high and the charge is homogeneous, such is not the case in zeolite X. In zeolite X, cesium atoms occupy several positions in the network at variable distances from oxygen. The population of

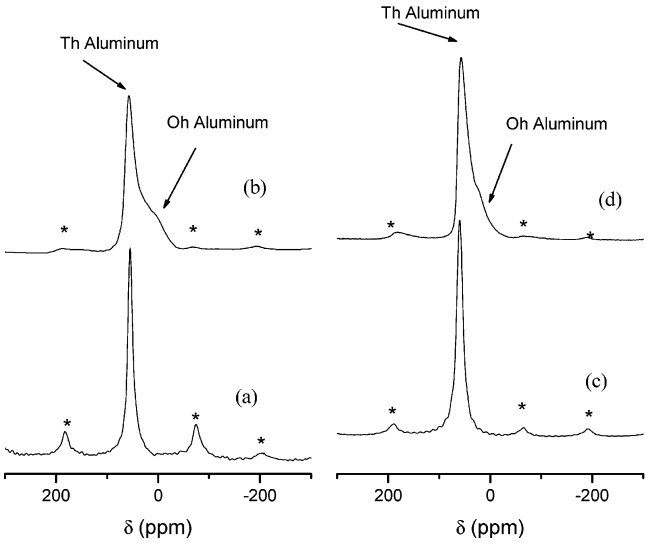

Figure 8. ^{27}Al MAS NMR spectra of zeolites (a) CsA-2 unheated, (b) CsA-2 heated at 1073 K, (c) CsX-2 unheated, and (d) CsX-2 heated at 973 K. Peaks labeled * are the spinning sidebands.

each site was determined by NMR, and it is found that the cesium acetate salt promotes a different positioning. This difference due to the anion of the cesium salt can only be understood in terms of the variation of acidity due to the radical CH_3COO^- which is the conjugated base of acetic acid CH_3-COOH, the corresponding ionization constant is $K_a = 1.8 \times 10^{-5}$ and the K_b is 5.6×10^{-10}. Although in very small amount, acetic acid is formed, the pH is changed and zeolite X wich is more fragile than zeolite A may hydrolyze. The corresponding calculated pH in our conditions is 8.9, experimentally we measured 8.6. In a previous work on cobalt exchange, we described how depending on time and the hydrolysis degree the cobalt species migrated and occupied different sites.[23,24]

XRD, FTIR, and ^{27}Al MAS NMR results show that zeolite lattice is modified when temperature is increased. Heating promotes the motion of cations into the free spaces of zeolite, as suggested by ^{133}Cs MAS NMR results (Tables 4 and 5). When the samples were heated at 673 K, all spectra in CsA series show that three types of site are occupied by cesium. The CsX-1 and the CsX-2 samples have also three types of site occupied, instead 4 types of site are occupied in the CsX-3 sample. Note that increasing the temperature from 298 to 673 K induces the migration of cesium from large cavities to sodalite cages.

When the samples are leached with the sodium chloride solution, high values of cesium retention are observed. The selectivity reported for a low exchange level (less than 40%) could explain this result:[25] Cs > Rb > K > Na. Hence, zeolites A or X retain cesium and do not exchange easily with sodium. Therefore, the exchanged ions should be those weakly bonded to the network, in our case the cations located in the large cavity. Experimentally, as shown by NMR, the exchanged cesium cations are indeed those in the large cavity (site II) which are more easily exchanged than cesium in position III, II′, and I′. Therefore, the position of cesium cations in the pores is a crucial parameter in the cesium retention.

Of course, then, the retained cesium, i.e., the cesium which remains in the zeolite network after being in contact with the NaCl solution, should not be distributed as initially. The cations of the large cavity have been exchanged. Table 5 includes the integrated intensities of the isotropic resonance of ^{133}Cs MAS NMR spectra recorded in dried leached samples. Clearly, the distribution of cesium in the sites of the zeolites is not the same before and after the leaching step. As a consequence of the leaching step the content of cesium in the zeolites is of course altered.

However, when the structure collapses, case of zeolite A heated at 1073 K, the cesium occupies only one site that has the same geometry before and after leaching step. This site clearly cannot be in zeolite A network because the remaining amount of zeolite is low in the mixture of A zeolite, nepheline, quartz, and amorphous material, and this mixture retains a high amount of cesium. Cesium located in nepheline is excluded because as it has been reported through thermodynamic calculations, the heats of hydration determine the selectivity sequence. The heat of hydration of sodium and cesium respectively $HaNa^+ = -423$ kJ/mol and $HaCs^+ = -280$ kJ/mol.[26] Cations with low hydration heats are preferred. In this sense, the studied zeolites are selective toward cesium. Then, the cesium has to be occluded in the amorphous material, which is an aluminosilicate where cesium is in a similar environment as in zeolites, but tighter, as in the corresponding radial distribution function the $Cs^+-O^=$ distance is shorter. Only in this material, cesium is immobilized, and no evidence, in the ^{133}Cs NMR spectra, of strong quadrupolar interactions is observed (no broadening of signals). Then, the factor determining the chemical shift observed should be the electric-field gradient generated in the adsorption site of cesium. This electric-field gradient is the result of the ordered charges in the environment of cesium, i.e, the

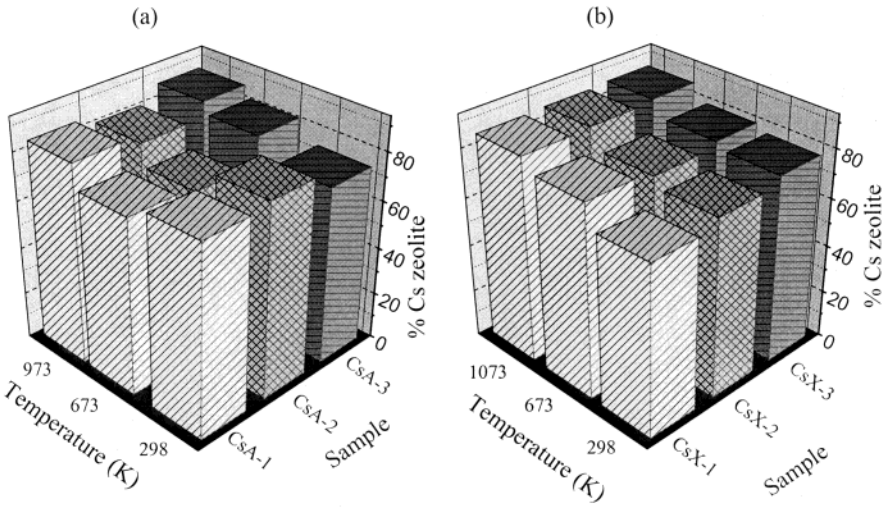

Figure 9. Cesium retained in zeolites after leaching step, (a) zeolites A and (b) zeolites X.

arrangement of oxygen, silicon, aluminum, and sodium ions in the space. The similar chemical shifts observed in the zeolitic material and in the mixture crystalline-vitreous material suggests that cesium in both materials is located in equivalent EFG. The EFG can be evaluated from ^{129}Xe and ^{131}Xe NMR.[27] We have tried to apply this method to calculate the EFG in our samples, unfortunately samples were unable to sorb xenon as this molecule cannot enter into the vitreous matrix due to its large size (0.44 nm) and reach cesium sites.

Note that such configurations have to agree with the radial distribution functions results, mainly with the shortening of Cs−O distances. From the obtained interatomic distances, the angles between (Al, Si)−O−(Al, Si) atoms can be estimated grosso modo as the distances (Al, Si)−O and (Al,Si)−(Al,Si) are provided. In both original zeolites, this angles is around 137°, after cesium exchange turns out to be 160−180° and after thermal treatment it becomes 170−185°. This configuration tends locally toward to spinel structure.

Conclusion

Depending on the anions present in the exchange solution, the cesium cations were found to be located in different sites of the zeolite, A or X, networks. If cesium acetate solution is used, cesium reaches sites SII and SIII in the large cavity whereas if nitrate or chloride solutions are put in contact with zeolites, cesium is positioned only in sites SIII. Cesium in the large cavity, sites II, leach out preferentially. When the samples were thermally treated to encapsulate partially the cesium cations, it was found that their behavior was different from the one observed in a previous work on cobalt exchanged X and A zeolites. NMR spectra and radial distribution functions show that with temperature, the local environment of cesium is significantly altered as cesium−oxygen distances is reduced. Non-leaching cesium in the thermally treated zeolite has to be occluded in an amorphous aluminosilicate network, where it maintains its original electric-field gradient.

Acknowledgment. The technical work of Leticia Baños is gratefully acknowledged.

References and Notes

(1) Armbruster T. *13th International Zeolite Conference*; Elsevier: Amsterdam, 2001.

(2) Gevorkyan, R.; Yeritsyan, H.; Keheyan, Y.; Sarkisyan, H.; Presutti, C.; Christidis, G.; Moraetis, D.; Kekelidze, N.; Akhalbeldashvili L. *13th International Zeolite Conference*; Elsevier: Amsterdam, 2001.

(3) Lima, E.; Bosch, P.; Bulbulian S. J. *Radioanal. Nucl. Chem.* **1998**, *237*, 41.

(4) Tsitsishvili, G. V.; Andronikashvili, T. G.; Kirov, G. N.; Filizova, L. D. *Natural Zeolites*; Ellis Horwood Limited: London, 1992.

(5) Giannetto, G.; Montes-Rendón, A.; Rodríguez-Fuentes, G. *Zeolitas, caracterización, propiedades y aplicaciones industriales*, Editorial Innovación Tecnológica, Facultad de Ingeniería: Caracas2000.

(6) Yamane I.; Nakazawa, T. Proc. *7th International Zeolite Conference*; Murakami., Y., Iijima, A., Ward, J. W., Eds.; Elsevier: Tokyo, 1986.

(7) Colella, C.; De'Gennaro, M.; Aiello R. *Rev. Min. Geochem*. **2001**, *45*, 551.

(8) Yu, J.-S.; Kevan, L. *J. Phys. Chem.* **1991**, *95*, 3262.

(9) Kalló D. In *Application of Natural Zeolites in Water and Wastewater Treatments*; Bish D. L., Ming D. W., Eds.; The Mineralogical Society of America: Washington, D.C., 2001; Vol 45.

(10) Becue, T.; Davis, R. J.; Garces, J. M. *J. Catal*. **1998**, *179*, 129.

(11) Solache, M.; García, I.; Bosch, P.; Bulbulian, S.; Blumenfeld A.; J. Fripiat. *Micr. Mater.* **1998**, *21*, 19.

(12) Thamzil, L.; *Waste Treatment Immobilization Technologies Involving Inorganic Sorbents*; International Atomic energy Agency: Vienna, 1997.

(13) Bulbulian, S.; Bosch P. *J. Nucl. Mater*. **2001**, *64*, 295.

(14) Dyer A., Abou-Jamous J. K., *J. Radional. Nucl. Chem.* **1997**, *59*, 224.

(15) Magini M.; Cabrini A., *J. Appl. Cryst*. **1972**, *29*, 702.

(16) Alvarez, L. J.; Ramirez-Solis, A.; Bosch-Giral P. *Zeolites* **1997**, *18*, 54.

(17) Hunger, M.; Schenk, U.; Burger, B.; Weitkamp, J. *Angew. Chem., Int. Ed. Engl*. **1977**, *36*, 2504.

(18) Norby, P.; Poshni, F. I.; Gualtieri, A. F.; Hanson, J. C.; Grey, C. P. *J. Phys. Chem. B* **1998**, *102*, 839.

(19) Malek, A.; Ozin,. G. A.; Macdonald, P. M. *J. Phys. Chem*. **1996**, *100*, 16 662.

(20) Flaningen, E. M.; Khatami, H.; Szymanski, H. A. *Adv. Chem. Ser.* **1971**, *101*, 201.

(21) Smirnov K. S., Bougeard D. *Catal. Today* **2001**, *70*, 243.

(22) Barrer, R. M.; Coughlan, B. *Molecular Sieves*; Society of Chemical Industry: London, 1986.

(23) García, I.; Solache-Ríos, M.; Bosch, P.; Bulbulian S. *J. Phys. Chem.* **1993**, *97*, 1249.

(24) Olguín, M. T.; Solache, M.; Iturbe, J. L.; Bosch, P.; Bulbulian, S. *Sep. Sci. Technol.* **1996**, *31*, 2021.

(25) Breck, D. W. *Zeolite Moleculer Sieves*; John Wiley: New York, 1974.

(26) Roque-Malherbe R. *Handbook of Surfaces and Interfaces of Materials*; H. S. Nalwa: New York, 2001.

(27) Millot, Y.; Man, P. *J. Magn. Res.* **2001**, *150*, 10.